J Therm Anal Calorim (2012) 110:385–394
DOI 10.1007/s10973-012-2308-4

Thermal analysis of tetraethylammonium and benzyltrimethylammonium montmorillonites

Shmuel Yariv · Isaak Lapides · Mikhail Borisover

CEEC-TAC1 Conference Special Issue

Abstract Na-montmorillonite was loaded with tetraethylammonium cations (TEA) or with benzyltrimethylammonium cations (BTMA) by replacing 77 and 81% of the exchangeable Na with TEA or BTMA, labeled TEA-MONT and BTMA-MONT, respectively. TEA- and BTMA-MONT were heated in air up to 900 °C. Thermally treated organoclays are used in our laboratory as sorbents of organic compounds from water. The two organoclays were studied by TG and DTG in air and under nitrogen. Carbon content in each of the heated sample was determined. They were diffracted by X-ray, and fitting calculations of d(001) peaks were performed on each diffractogram. TG and thermo-C analysis showed that at 150 and 250 °C both organoclays lost water but not intercalated ammonium cations. DTG peak of the first oxidation step of the organic cation with the formation of low-temperature stable charcoal (LTSC) appeared at 364 and 313 °C for TEA- and BTMA-MONT, respectively. The charcoal was gradually oxidized by air with further rise in temperature. DTG peak of the second oxidation step with the formation of high-temperature stable charcoal (HTSC) appeared at 397 and 380 °C for TEA- and BTMA-MONT, respectively. DTG peak of the final oxidation step of the organic matter appeared at 694 and 705 °C for TEA- and BTMA-MONT, respectively, after the dehydroxylation of the clay. Thermo-XRD analysis detected TEA-MONT tactoids with spacing 1.40 and 1.46 nm up to 300 °C. At 300 and 360 °C, LTSC-MONT tactoids were detected with spacing of 1.29 nm. At higher temperatures, HTSC-MONT-α and -β tactoids were detected with spacings of 1.28 and 1.13 nm, respectively. BTMA-MONT tactoids with spacings 1.46 and 1.53 nm were detected up to 250 °C. At 300 and 360 °C, LTSC-MONT tactoids were detected with a spacing of 1.38 nm. At higher temperatures, HTSC-MONT-α and -β tactoids were detected with spacings of 1.28 and 1.17 nm, respectively. At 650 °C, both clays were collapsed. HTSC-β-MONT differs from HTSC-α-MONT by having carbon atoms keying into the ditrigonal holes of the clay-O-planes. At 900 °C, the clay fraction is amorphous. Trace amounts of spinel and cristobalite are obtained from thermal recrystallization of amorphous *meta*-MONT.

Keywords C content · Charcoal · Organo-montmorillonite · Thermogravimetry · Tactoids · Thermal analysis · X-ray

Introduction

Organoclay-based nanocomposites obtained by modifying Na-smectites with quaternary ammonium cations are potential candidates for serving as sorbents of different organic molecules [1–3] and are used in cleaning operations of drainage wastewater, oil-spill, etc. [4–8]. The adsorption of the organic molecules by the quaternary ammonium clay is known as a secondary adsorption. In recent years, our research has been focused on the effect of thermally treating the ammonium clay on its secondary adsorption ability of organic molecules from water. The

Dedicated to Prof. G. Liptay on the occasion of his 80th birthday.

S. Yariv (✉) · I. Lapides
Institute of Chemistry, The Hebrew University of Jerusalem, Edmund Y. Safra Campus, 91904 Jerusalem, Israel
e-mail: yarivs@vms.huji.ac.il

M. Borisover
Institute of Soil, Water and Environmental Sciences, The Volcani Center, POB 6, 50250 Bet Dagan, Israel

quaternary ammonium cation used in our previous work was hexadecyltrimethylammonium (HDTMA) and the clay mineral was montmorillonite (MONT).

Secondary adsorption of nitrobenzene on HDTMA-MONT from an aqueous solution was studied [9]. The substrate was heated 2 h in air at 150, 250, 360, and 420 °C. Mild heating of sorbent (at 150 °C) resulted in a distinct increase of the secondary adsorption efficacy probably associated with the escape of interlayer water. Treatment of organoclay at higher temperatures (250 and 360 °C) resulted in the first oxidation step of intercalated HDTMA. This had a little impact on the sorption efficacy as compared with organoclays treated at 150 °C. Further increase of the treatment temperature (420 °C) resulted in a decrease of the sorption efficacy. Mild heating of organoclays in air could be useful for improving their adsorption potential.

Hexadecyltrimethylammonium is a quaternary ammonium with a long chain. Recently, we studied the effect of sorbent heating on the secondary adsorption of nitrobenzene from aqueous solutions on MONT modified by quaternary ammonium cations with no long chains [10]. The quaternary ammonium cations used in that work were tetraethylammonium (TEA) and benzyltrimethylammonium (BTMA), (Schemes 1, 2), and the clay mineral was MONT heated 2 h in air at 150, 360, and 420 °C. Mild heating of sorbents (at 150 °C) resulted in a distinct increase of the secondary adsorption efficacy. Treatment at 360 °C produced a sorbent more effective than the non-heated but demonstrating worse removal of nitrobenzene from water as compared with the TEA-MONT or BTMA-MONT treated at 150 °C. Sorption of nitrobenzene on both organo-MONT preheated at 420 °C was similar to those on the non-heated sorbents.

Thermal analyses of organic matter in soils and of organoclays (mainly organo-MONTs) in air have been widely investigated and reviewed (see, e.g. [11–17]). Although the shapes of the thermal analysis curves depend on the organic compound and on the extent of adsorption, with most organoclays three different steps of the oxidation of the organic matter were identified by simultaneous DTA, DTG, and EGA [18]. In the first oxidation step, H_2O is the principal evolved gas obtained from the oxidation of the hydrogen atoms of the organic matter. This water is termed "organic water". At this step, relatively small amounts of CO_2 and NO_2 are also evolved. Carbon and nitrogen atoms, which do not take part in the formation of the gaseous volatile oxides, together with very small amounts of hydrogen atoms which were not oxidized form a black intercalated residue, known as petroleum coke or charcoal [19, 20]. In the second oxidation step, part of the charcoal is oxidized to CO_2 and NO_2. The fraction which is oxidized at this step is named "low-temperature stable charcoal" (LTSC). In the third oxidation step, the rest of charcoal is oxidized to CO_2 and NO_2. The fraction of charcoal which is oxidized at this step is named "high-temperature stable charcoal" (HTSC). The last oxidation steps of the HTSC occur simultaneously with the dehydroxylation of the clay and its transformation into amorphous *meta*-MONT. After the oxidation of the HTSC, the fraction of MONT which did not dehydroxylate became collapsed. In conclusion, as a consequence of the thermal reactions of the intercalated organic matter, the clay products which are obtained in the three steps are: (1) LTSC-MONT, (2) HTSC-MONT, and (3) collapsed and amorphous *meta*-MONT, respectively.

Scheme 1 Tetraethylammonium cation $(TEA)^+$

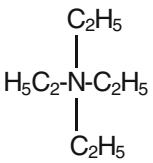

Scheme 2 Benzyltrimethylammonium cation $(BTMA)^+$

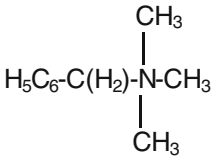

Very little is known on the structure and properties of charcoal–clay. In order to apply these composite nanocomplexes in different technologies, more information on their structures and properties are required. During thermal analysis of HDTMA-MONT (DTG, thermo-C and H analyses, thermo-IR-spectroscopy analysis, and thermo-XRD analysis), three types of intercalation charcoal-MONT complexes were identified: (1) LTSC-MONT tactoids with a basal spacing 1.32–1.39 nm, between 250 and 420 °C; (2) HTSC-α-MONT tactoids with spacing 1.22–1.28 nm, between 360 and 550 °C; and (3) HTSC-β-MONT with spacing 1.12–1.18 nm, between 250 and 550 °C. HTSC-β-MONT differs from HTSC-α-MONT by having carbon atoms keying into the ditrigonal holes of the clay-O-planes [21, 22]. In the present study, the thermal analysis of TEA-MONT and BTMA-MONT is investigated by TG–DTG, thermo-C analysis, and thermo-XRD analysis. Thermo-IR-spectroscopy analysis of the samples was previously described [10].

Experimental

Materials

Wyoming bentonite (Na-montmorillonite rich clay [23]) with cation exchange capacity (CEC) of 90.7 meq/100 g

was obtained from Fisher Scientific (U.S.). This clay was characterized earlier using XRD [9], DTA/TG/DTG [13], and thermo-C/H analyses [21, 22]. TEA chloride hydrate and BTMA chloride (both 98%) were purchased from Sigma-Aldrich and used without further purification.

Preparation and characterization of organoclays

The preparation of TEA-MONT and BTMA-MONT was previously described [10]. In brief, 3 L of homogeneous 1.5% w/w aqueous bentonite suspension was prepared by continuous stirring during 4 h. Then, 1 L of the aqueous solution containing 0.044 mol/L of TEA chloride or 0.064 mol/L of BTMA chloride was added, with the rate of 1.0–1.5 mL/min. Nominal ratio of organic cation added (per 100 g of clay) to the clay CEC was 1.08 and 1.58 for TEA and BTMA, respectively. After additional overnight stirring, suspension of the organo-MONT was centrifuged, washed repeatedly with distilled water until negative reaction with $AgNO_3$. Thermal treatment of synthesized organoclays involved heating during 2 h at 150, 250, 300, 360, 420, 500, 550, 650, 700, and 900 °C in an oven (in air). After heating, the sorbents were kept in a desiccator. Based on C contents of freeze-dried synthesized organoclays, the extent of cation exchange (relative to CEC) was determined as 77% for TEA-MONT and 81% for BTMA-MONT.

Thermogravimetric analyses

TG and DTG curves of 8–15 mg of Na-MONT, TEA-MONT, and BTMA-MONT were recorded from room temperature to 900 °C on a thermobalance Mettler Toledo TG50 analyzer. Measurements were performed at a heating rate of 10 °C/min. Parallel runs were carried out in air and in nitrogen atmosphere. The DTG curves of the organoclays measured in air were fitted in the temperature range 225–475 °C using "Origin 7.0" program.

Thermo-C analysis

Carbon contents of Na-MONT, TEA-MONT, and BTMA-MONT unheated and after thermal treatments were determined at the Laboratory for Micro-Analysis of the Institute of Chemistry at the Hebrew University of Jerusalem using a Perkin-Elmer-2400 C/H analyzer. Portions of 2–3 mg sample were used for each run.

Thermo-XRD analysis

In the present thermo-XRD analysis study, the effect of the thermal treatment on the basal spacings of the organoclay was determined [24]. X-ray diffractograms of powder samples of unheated and thermally treated TEA-MONT and BTMA-MONT were recorded at room temperature, under ambient atmosphere, using a Philips Automatic Diffractometer (PW 1710) with a Cu tube anode. Peak d(001) in diffractograms recorded during the thermo-XRD analysis was fitted by "PHILIPS" Automatic Powder Diffraction (PW1877/43) software, version 3.5. Profile fitting was used for accurate determination of peak positions, widths, backgrounds, and intensities (relative peak component areas). Gaussian shapes were used for the peaks. The fitting method was previously described [25].

Results and discussions

TG and DTG curves

TG and DTG curves of Na-MONT, TEA-MONT, and BTMA-MONT recorded in air atmosphere are shown in Fig. 1 (curves a, b, and d, respectively) together with the DTG curve fitting calculations in the temperature range 200–475 °C (curves c and e, respectively). The DTG curve of Na-MONT (previously published [21]) shows two peaks at 100 and 685 °C suggesting the presence of two thermal stages of mass loss due to the escape of interlayer water and the dehydroxylation of the clay, respectively. The DTG curves of both organoclays, together with the fitted DTG curves, show five peaks suggesting the presence of five thermal stages of mass loss. In the curve of TEA-MONT, they appear at 51, 364, 397, 610, and 694 °C and in that of BTMA-MONT at 62, 313, 380, 610, and 705 °C. The first DTG peak occurs with the escape of interlayer water. First

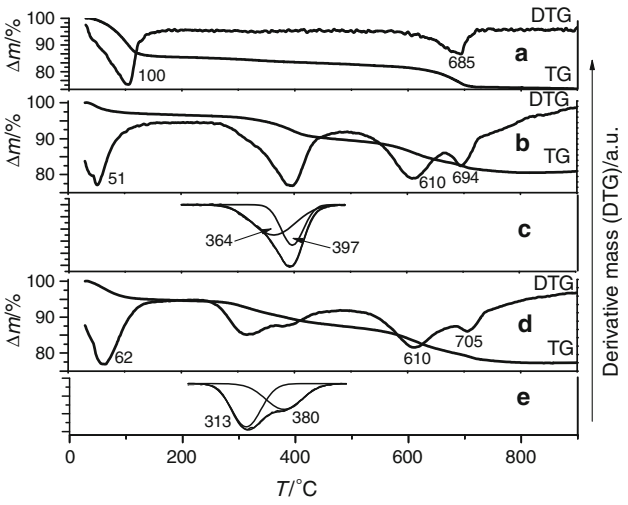

Fig. 1 TG and DTG curves recorded in air of Na-MONT (*curve a*), TEA-MONT (*curves b* and *c*), and BTMA-MONT (*curves d* and *e*). *Curves a, b,* and *d* TG and DTG curves; *curves c* and *e* fitted DTG curves in the temperature range 200–475 °C

stage mass losses (25–250 °C) determined in Na-MONT [26], TEA-MONT, and BTMA-MONT are 10.5, 3.6, and 5.6%, respectively. These results indicate that the amount of interlayer water decreases as a result of the adsorption of organic matter.

In air the second thermal mass loss stage results from the first oxidation step of the organic cation, the escape mainly of organic H_2O and to a small extent also CO_2 and NO_2 and the formation of non-volatile intercalated charcoal (LTSC). The second DTG peak occurs in TEA-MONT at a higher temperature than in BTMA-MONT, indicating that charcoal formation in the former occurs at a higher temperature.

The third thermal mass loss stage comprises the oxidation of the LTSC leaving the HTSC variety in the clay interlayer (the second oxidation step of the organic cation). Here again the third DTG peak occurs in TEA-MONT at a higher temperature than in BTMA-MONT. The fourth mass loss stage (fourth DTG peak) represents the dehydroxylation of the clay. As shown previously, organic-ammonium-MONTs dehydroxylate at temperatures lower than neat Na-MONT [27–30]. The fifth mass loss stage (fifth DTG peak) represents the oxidation of the HTSC (the third oxidation step of the organic cation). It appears in the DTG curve of TEA-MONT at a lower temperature than in that of BTMA-MONT.

The TG curves of TEA-MONT and BTMA-MONT show overlapping of mass loss in the second and third stages, on one hand, and in the fourth and fifth stages, on the other. Mass losses in these overlapping stages (250–490 °C and 490–800 °C, respectively) are 6.8 and 9.1% in the TG curve of air-dried TEA-MONT (or 8.5 and 11.4% in TG of TEA-MONT calcined at 900 °C) and 6.9 and 10.1 in the TG curve of air-dried BTMA-MONT (or 9.0 and 12.6% in TG of BTMA-MONT calcined at 900 °C). Air-dried Na-MONT shows mass loss in the equivalent temperature ranges 250–490 and 490–800 °C of 1.7 and 4.9%, respectively (or 2.3 and 6.7% in TG of Na-MONT calcined at 900 °C) [26]. The last mass loss of Na-MONT results from the dehydroxylation of the clay. The oxidation of HTSC in TEA-MONT and BTMA-MONT overlaps the dehydroxylation of the clay. Consequently, the percent of HTSC is determined by subtracting 4.9% from the mass loss occurring in the fourth and fifth stages of air-dried clays (or 6.7% from mass loss of calcined clays). It is equal to 4.2 and 5.2% in air-dried TEA-MONT and BTMA-MONT, respectively (or 4.7 and 5.9% in calcined TEA-MONT and BTMA-MONT, respectively).

A careful examination of TG curves of TEA-MONT and BTMA-MONT shows inflections at 380 and 370 °C. These data indicate that mass loss in the first oxidation step is 3.4 and 4.0% and in the second step is 3.6 and 3.1%, respectively. However, these numbers should be taken in cautious because of the overlapping of the two oxidation steps.

Thermal degradation of different organoclays in inert atmosphere was investigated by several investigators [31–36]. Thermal analysis curves of organoclays show stepwise degradation which corresponds to residual water desorption followed by decomposition of the organic modifier and volatilization of organic fragments, dehydroxylation of the clay and the last stages of organic matter degradation and volatilization. Depending on the adsorbed organic species, simultaneous TG–EGA showed three, two, and one well-defined degradation stages. It was also observed that the onset of the decomposition was different for each type of organoclay and also depended on whether the organic species was adsorbed on the outside surface or inside the interlayer. Mass and IR spectra of the evolved gases showed the presence of water, aldehydes, carboxylic acids, aliphatic compounds and in some cases also aromatic compounds and CO_2.

The DTG curve of TEA-MONT recorded under nitrogen (Fig. 2b) shows four distinct peaks at 53, 445, 614, and 645 °C and a very broad weak peak at 803 °C, representing (1) dehydration, (2) thermal degradation of TEA cations followed by the escape of volatile fragments and the condensation of nonvolatile fragments into some kind of quasi-charcoal, and (3) dehydroxylation of the clay and in the last two stages the pyrolysis of the quasi-charcoal. The TG curve shows that the peaks are associated with mass losses of 4.0% (25–215 °C, dehydration), 10.6% (215–525 °C), 4.2% (525–720 °C), and 1.0% (700–900 °C), respectively.

DTG curve of BTMA-MONT recorded under nitrogen (Fig. 2c) shows five peaks at 54, 352, 413, 583, and 631 °C, and a very broad weak peak at 794 °C, representing (1) dehydration, (2, 3) degradation of BTMA, escape of volatile fragments and condensation of the residue, (4) dehydroxylation of the clay and (5, 6) pyrolysis of

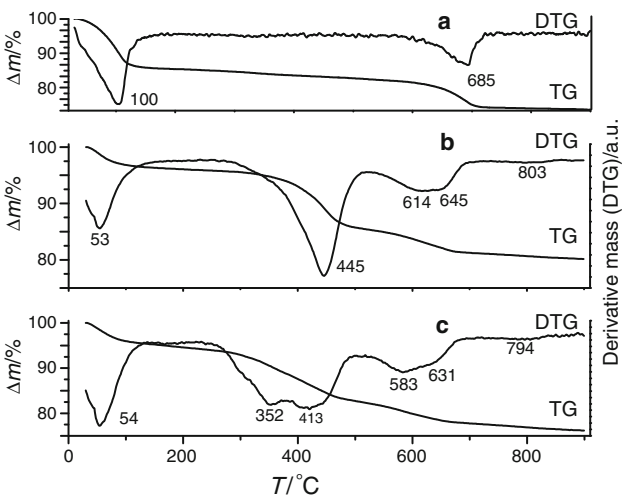

Fig. 2 TG and DTG curves recorded under nitrogen of Na-MONT (*curve a*), TEA-MONT (*curve b*), and BTMA-MONT (*curve c*)

Table 1 Carbon content (in % w/w) in non-heated and in thermally treated samples of TEA-MONT and BTMA-MONT

Temperature/°C	TEA-MONT/%	BTMA-MONT/%
25	6.7	8.6
150	6.8	8.3
250	7.0	8.3
300	5.6	5.5
360	3.1	4.1
420	3.0	3.2
500	1.9	2.2
550	1.1	1.4
650	0.2	0.3
700	0.1	0.1

the quasi-charcoal to volatile fragments. The TG curve shows that the peaks are associated with mass losses of 5.6% (25–215 °C), 5.4% (215–375 °C), 6.4% (375–510 °C), 4.9% (510–710 °C), and 1.5% (710–900 °C), respectively. Dehydration mass losses recorded under nitrogen are similar to those recorded under air. The results under air or under nitrogen indicate that the amount of interlayer water decreases as a result of the adsorption of organic matter. BTMA-MONT contains higher amounts of interlayer water than TEA-MONT.

In conclusion, two types of charcoal are identified from the TG and DTG curves recorded in air. They are LTSC and HTSC. They are oxidized during the second and third steps of air oxidation, respectively.

Thermo-C analysis

Carbon contents determined in each clay sample by micro-analysis before and after thermal treatments are shown in Table 1. The thermal treatments were carried out in steps. The nature of this thermal treatment differs from that used in the TG–DTG study, where the samples were consecutively heated from room temperature to 900 °C. It should be taken into consideration that a reaction attributed to a certain DTG peak might be completed in the non-consecutive thermal treatment at a lower temperature.

The content of carbon in Na-MONT is 1.0% due to the presence of some organic impurities in the Wyoming bentonite. Before the thermal treatments, the contents of carbon in TEA-MONT and BTMA-MONT are 6.7 and 8.6%, respectively. The table shows negligible differences of 0.1 and 0.3% at 150 and 250 °C which are probably due to experimental inaccuracy or non-homogeneity of the samples. From data in Table 1, it is obvious that both TEA-clay and BTMA-clay begin to lose C only after heating at temperatures exceeding 250 °C. In the first step of the air oxidation of adsorbed amines, organic water is the principal gas which evolves. It is formed by the oxidation of the organic hydrogen atoms. Some CO_2, which is formed by the oxidation of some organic carbon atoms, also evolves. The non-evolved carbon atoms form intercalated non-volatile charcoal [18].

A small decrease in carbon content of 1.4% (20.0% from total C) occurs in TEA-MONT during heating from 250 to 300 °C. On the other hand, the thermo-carbon analysis of BTMA-MONT shows during heating from 250 to 300 °C a higher carbon decrease of 2.8% (32.6% from total C). At 300 °C, oxidation of the organic cation and formation of LTSC is significant in the latter, but is small in the former. This is supported by the locations of the peak of the first oxidation step in the DTG curves of TEA-MONT and BTMA-MONT. They are at 364 °C in the former and at 313 °C in the latter. The great carbon mass loss determined for BTMA-MONT may suggest that much of the LTSC formed at this thermal treatment is further oxidized. As we are going to show in section "Thermo-XRD analysis", this sample contains also HTSC-MONT.

During heating from 300 to 360 °C, carbon content further drops in TEA-MONT and in BTMA-MONT by 2.5 and 1.4% (35.7 and 16.3% from total C), respectively. At this temperature, oxidation and existence of charcoal are evident in both samples from the IR spectra [10]. In agreement with the DTG observations, the present results confirm that the first and second oxidation steps of the organic cation in TEA-MONT occur at higher temperatures than those steps in BTMA-MONT.

During heating from 360 to 420 °C, carbon content drops slightly by 0.1% in TEA-MONT (1.4% from total C) and much more by 0.9% in BTMA-MONT (10.5% from total C). The small decrease in carbon in the former is probably due to the oxidation of LTSC which has not been oxidized at 360 °C, whereas the significant decrease in the latter is due to the beginning of the oxidation of HTSC. During heating from 420 to 500 °C, carbon content further drops in TEA-MONT by 1.1% (15.7% from total C) and in BTMA-MONT by 1.0% (11.6% from total C). At this thermal treatment, part of HTSC is oxidized in both clay samples.

At and above 500 °C, there is a continuous decrease in carbon content. Carbon loss at 500–900 °C is due to the oxidation of HTSC [12, 18]. Heating the samples from 500 to 550 °C leads to a carbon content decrease by 0.8% in both clays (11.4 and 9.3% from total C in TEA- and BTMA-MONT, respectively). During heating from 550 to 650 °C, carbon content further drops by 0.9 and 1.0% (12.9 and 11.6% from total C) in TEA- and BTMA-MONT, respectively. By further heating from 650 to 700 °C, carbon content further drops by 0.1 and 0.2% (1.4 and 2.3% from total C) in TEA- and BTMA-MONT, respectively. In agreement with the DTG observations, the present results

confirm that the completion of the oxidation of HTSC in BTMA-MONT requires a higher temperature than that in TEA-MONT. After heating both samples at 900 °C, carbon content is beyond the determination limit.

In conclusion, thermo-C analysis demonstrates the existence of two types of charcoal. LTSC is oxidized at temperatures below 420 and 360 °C, in TEA-MONT and in BTMA-MONT, respectively, whereas HTSC is oxidized at higher temperatures.

Thermo-XRD analysis

The curve fitting calculations on most X-ray diffractograms result in two peak components. Only the fitting of TEA-MONT heated at 300 °C results in three peak components. Each peak component characterizes one type of tactoids (clusters composed of several parallel face-to-face TOT layers). Maximum location (in nm) describes the basal spacing of the respective tactoid. Relative peak component area (in percent from the total peak area) shows the relative concentration of the respective tactoid in the stack. The width of the peak component (in °2θ) represents the homogeneity of the respective tactoid. A homogeneous stack of tactoids poses a narrow component width, whereas an inhomogeneous stack poses a broad width. Only calculations with χ^2 within the range between 0.24 and 0.35 (where χ^2 is a statistical term) which are supposed to be reasonable, are taken into consideration in the present study.

Two types of intercalated charcoal are identified from our TG curves and the thermo-C analysis, namely, LTSC and HTSC, respectively. In our previous thermo-XRD analysis study of HDTMA-MONT, we identified by XRD two types of MONT tactoids intercalated by HTSC, with spacings of $\approx$1.25 and $\approx$1.15 nm. They were labeled by α and β, respectively. The $\approx$1.25 nm allows the tactoid to intercalate carbon monolayers, whereas $\approx$1.15 nm requires the penetration (keying) of the carbon atoms into the ditrigonal holes of the clay-O-planes [22]. In the present thermo-XRD analysis, we are going to show that XRD of TEA- and BTMA-MONT also identifies two types of tactoids of intercalated HTSC.

Results of curve fitting calculations on diffractograms recorded during thermo-XRD analysis of air-dried powders of TEA- and BTMA-MONT are depicted in Tables 2 and 3, respectively. Columns in the tables describe the MONT complexes which are expected to exist at the certain temperature, based on the present TG–DTG and thermo-C analysis and on thermo-IR-spectroscopy study which was previously described [10].

Basal spacings of freeze-dried TEA-MONT and BTMA-MONT are 1.36 and 1.45 nm, respectively [10]. Curve fitting calculations on the diffractograms of unheated air-dried TEA-MONT and BTMA-MONT result in two peak components with maxima at 1.46 and 1.40 nm (Table 2) and at 1.53 and 1.46 nm (Table 3), respectively, indicating in each ammonium clay the presence of two types of tactoids labeled A and B, respectively. The differences between the freeze- and air-dried samples suggest that the presence of water in the interlayer affects the arrangement of the organic cation in the interlayer of the clay. Assuming similar diffraction indices to both tactoids, from relative peak component areas it appears that in air-dried TEA-MONT tactoids of type A, with the larger spacing, comprise 42% of the stack whereas those of type B comprise 58%. In air-dried BTMA-MONT tactoids of type A, with the larger spacing, comprise 29% of the stack whereas those of type B comprise 71%. All these spacings allow the presence of intercalated lateral monolayers of TEA or BTMA. In TEA-MONT-A, the C_2H_5 chains are probably lying more tilted relative to the clay-O-plane than in B. The peak components, with width at half heights of 0.76 and 0.38 °2θ, respectively, indicate that tactoids B are more homogeneous than tactoids A. In BTMA-MONT-A, the C_6H_5 rings are probably lying more tilted relative to the clay-O-plane than in B. The peak components, with width at half heights of 0.79 and 0.40 °2θ, respectively, indicate that tactoids B are more homogeneous than tactoids A. Both widths calculated from the diffractograms of TEA-MONT A and B are similar to those calculated from the diffractograms of BTMA-MONT A and B, respectively, but are smaller than that calculated previously from the diffractogram of Na-MONT (2.83 °2θ), indicating that tactoids of both types of TEA-MONT or BTMA-MONT are more homogeneous than those of Na-MONT.

Only minor changes in basal spacings, relative component areas, and component widths at half heights are observed after heating TEA-MONT at 150 and 250 °C, which may result from the inaccuracy of the curve fitting calculations (Table 2). This is in agreement with the TG–DTG, thermo-C analysis, and thermo-IR-spectroscopy [11] which show that the first step oxidation of intercalated TEA occurs at above 250 °C. At 300 °C, a new peak component appears with spacing of 1.29 nm, attributed to tactoids of LTSC-MONT, comprising only 10% of the clay stack. This spacing characterizes tactoids with intercalated monolayers of carbon atoms lying parallel to the clay-O-plane. In addition to LTSC-MONT, the clay stack contains non-oxidized TEA-MONT varieties A and B. The concentration of variety A decreases during the thermal treatment (Table 2), suggesting that at this stage mainly this variety is transformed into LTSC-MONT.

In the DTG curve of TEA-MONT (Fig. 1c), a peak attributed to organic H oxidation and formation of charcoal appears at 364 °C. In agreement with this observation, after heating at 360 °C the relative concentration of LTSC-MONT increases to 93%. In the present case, spacings of LTSC-MONT and HTSC-MONT-α are similar (1.29 and

Table 2 Summary of curve fitting calculations on diffractograms of thermo-XRD analysis of air-dried tetraethylammonium-montmorillonite, *top*, maxima of peak components (in nm), *middle*, relative component area (in % of the total peak area), and *bottom*, component width at half heights (in °2θ)

Heating temp./ °C	TEA-MONT-A	TEA-MONT-B	LTSC-MONT	HTSC-α-MONT	HTSC-MONT-β	Partial collapsed	Fully collapsed
Maxima of peak components/nm							
25	1.46	1.40					
150	1.48	1.39					
250	1.47	1.41					
300	1.46	1.40	1.29				
360			1.29		1.11		
420				1.28	1.11		
500				1.28	1.15		0.99
550					1.15	1.02	0.97
650						1.02	0.97
700						1.03	0.97
Relative component area (in % of the total peak area; concentration of the respective tactoid in the clay stack)							
25	42	58					
150	35	65					
250	46	54					
300	29	61	10				
360			93		7		
420				86	14		
500				31	59		10
550					38	43	19
650						28	72
700						34	66
Component width at half heights/°2θ							
25	0.76	0.38					
150	0.71	0.39					
250	0.77	0.32					
300	1.03	0.51	1.24				
360			1.92		1.20		
420				2.16	1.32		
500				2.70	1.92		0.68
550					1.96	1.07	0.79
650						0.92	0.48
700						1.16	0.47

1.28 nm) and X-ray does not differentiate unequivocally between them. It is possible that the sample contains also HTSC-MONT-α. Small amounts (7%) of HTSC-MONT-β are also detected (Table 2).

In the DTG curve of TEA-MONT, the peak attributed to the oxidation of LTSC appears at 397 °C (Fig. 1c). Consequently, the sample heated at 420 °C should not contain LTSC but only HTSC. The curve fitting calculations result in two peak components at 1.28 and 1.11 nm (Table 2), attributed to HTSC-α-MONT and HTSC-β-MONT, respectively. Table 2 shows that HTSC-α-MONT is present also at 500 °C, but its concentration decreases when heated from 420 to 500 °C. On the other hand, concentration of HTSC-β-MONT increases. At 550 °C, HTSC-β-MONT is present together with collapsed clay but only collapsed clay is present at 650 and 700 °C. It should be noted that at these temperatures most of the clay is dehydroxylated and is amorphous and does not diffract X-ray. The peaks at 1.02 and 0.97 nm are attributed to the small amounts of non-dehydroxylated clay fraction. According to Table 1, these samples still contain very small amounts of carbon.

Only small change in basal spacing is observed after heating BTMA-MONT at 150 or 250 °C, which may result from the inaccuracy of the curve fitting calculations. This is

Table 3 Summary of curve fitting calculations on diffractograms of thermo-XRD analysis of air-dried benzyltrimethylammonium-montmorillonite, *top*, maxima of peak components (in nm), *middle*, relative component area (in % of the total peak area), and *bottom*, component width at half heights (in °2θ)

Heating temp./ °C	BTMA-MONT-A	BTMA-MONT-B	LTSC-MONT	HTSC-α-MONT	HTSC-MONT-β	Partial collapsed	Fully collapsed
Maxima of peak components/nm							
25	1.53	1.46					
150	1.54	1.46					
250	1.52	1.47					
300			1.36	1.29			
360			1.40	1.29			
420				1.27		1.05	
500					1.18	1.02	
550					1.16	1.02	
650						1.07	0.98
700						1.05	0.97
Relative component area (in % of the total peak area; concentration of the respective tactoid in the clay stack)							
25	29	71					
150	32	68					
250	39	61					
300			51	49			
360			31	69			
420				95		5	
500					69	31	
550					29	45	
650						38	62
700						31	69
Component width at half heights/°2θ							
25	0.79	0.40					
150	0.81	0.40					
250	0.95	0.40					
300			1.23	1.02			
360			1.18	0.97			
420				1.54		1.41	
500					2.37	1.17	
550					1.14	1.11	
650						1.91	0.92
700						1.32	0.52

in agreement with the TG–DTG, thermo-IR analysis, and thermo-C analysis, which show that the first step oxidation of BTMA occurs at above 250 °C. However, the relative component area of BTMA-MONT A increases with the temperature suggesting that variety B of BTMA-MONT is transformed to A with the escape of interlayer water.

In the DTG curve of BTMA-MONT (Fig. 1e), the peak attributed to organic H oxidation and formation of charcoal appears at 313 °C. In agreement with this observation, after heating the sample at 300 °C two new peak components appear with spacings 1.36 and 1.29 nm (Table 3), attributed to tactoids of LTSC-MONT and HTSC-α-MONT, comprising 51 and 49%, respectively, of the clay stack. Both spacings characterize intercalated monolayers of carbon atoms lying parallel to the clay-O-plane, in the latter the layer being more compact than in the former.

After heating at 360 °C, the relative concentration of LTSC-MONT decreases to 31% and that of HTSC-MONT increases to 69% (Table 3). The width of the peak components shows that the homogeneity of the latter is higher than that of the former.

In the DTG curve of BTMA-MONT, the peak attributed to LTSC oxidation appears at 380 °C. Consequently, the sample heated at 420 °C should not contain LTSC-MONT but only HTSC-MONT. The curve fitting calculations result in two peak components at 1.27 and 1.05 nm, attributed to HTSC-α-MONT and partially collapsed clay, with component areas 95 and 5%, respectively. From the width of the 1.27 nm peak component, it is shown that the homogeneity of HTSC-α-MONT is poor. It is possible that some tactoids of HTSC-β-MONT are also present in the stack leading to the broadening of the peak component.

HTSC-α-MONT is not detected after heating at 500 °C and at higher temperatures. HTSC-β-MONT is present after heating at 500 and 550 °C together with partially collapsed clay but its concentration decreases when heated from 500 to 550 °C and it is not detected at 650 and 700 °C. At these temperatures, only partially and fully collapsed clays are detected. According to Table 1, these samples still contain some carbon. We assume that carbon atoms are present in the interlayer space, keying into the ditrigonal holes of the clay-O-planes and thus preventing the full collapse of the clay to occur.

After heating Na-MONT, TEA-MONT, and BTMA-MONT at 900 °C, the clay fraction becomes amorphous and MONT peaks do not appear in the diffractograms. Trace amounts of spinel and cristobalite are obtained from thermal recrystallization. Quartz is present as an impurity in the Wyoming bentonite and after the amorphization of MONT its X-ray peak becomes very intense. There are no significant differences between the diffractograms of the three clays. Our results are in good agreement with previous studies of thermal treatment of Na-MONT [37].

Conclusions

Formation of LTSC and HTSC during the thermal treatments of TEA-MONT and BTMA-MONT is shown from TG–DTG and thermo-C analysis studies. During the thermo-XRD analysis of both organoclays, combined with curve fitting calculations on the diffractograms, the following spacings are used for the identification of the different tactoids. Spacings of TEA-MONT A or B tactoids are 1.46 or 1.40 nm, respectively. In the thermo-XRD analysis, they are identified in samples heated up to 300 °C. Spacings of BTMA-MONT A or B tactoids are 1.46 or 1.53 nm, respectively. In the thermo-XRD analysis, they are identified in samples heated up to 250 °C. Three types of charcoal-MONT complexes are identified: (1) spacings of LTSC-MONT tactoids obtained by heating TEA-MONT or BTMA-MONT are 1.29 or 1.38 nm, respectively. They are detected in both organoclays heated at 300 °C (10 and 51% from total clay fraction, respectively) or 360 °C (69 and 31%, respectively); (2) spacings of HTSC-α-MONT tactoids obtained by heating TEA-MONT or BTMA-MONT are 1.28 nm. They are identified after heating the former at 420 or 500 °C (86 and 31%, respectively) and the latter at 300, 360, or 420 °C (49, 69, and 95%, respectively); (3) spacings of HTSC-β-MONT tactoids obtained by heating TEA-MONT or BTMA-MONT are 1.13 or 1.17 nm, respectively. They are identified after heating the former at 360, 420, 500, or 550 °C (7, 14, 59, and 38%, respectively) and the latter at 500 or 550 °C (69 and 29%, respectively). Incomplete collapsed tactoids are identified by a maximum at 1.02-1.07 nm. They occur between 550–700 and 420–700 °C in the thermal analysis of TEA-MONT or BTMA-MONT, respectively. Fully collapsed tactoids are characterized by a maximum at 0.97–0.99 nm. They occur at 700 °C.

Spacing of 1.28 nm permits the intercalation of a monolayer of carbon atoms lying parallel to the clay layers. A shorter spacing does not permit this arrangement in the interlayer. It is therefore assumed that HTSC-β-MONT differs from HTSC-α-MONT by having carbon atoms keying into the ditrigonal holes of the clay-O-planes.

A fully collapsed montmorillonite obtained from the dehydration of Na-MONT has a spacing of 0.97 nm. It is expected that during the collapse non-hydrated exchangeable Na cations penetrate through the ditrigonal holes of the clay-O-plane into the tetrahedral sheets. The presence of carbon in TEA-MONT and BTMA-MONT heated at 650 and 700 °C is determined by C analysis (Table 1). These carbon atoms which are present in the interlayer space are keying into the ditrigonal holes of the clay-O-planes and thus preventing the full collapse of the clay. Consequently, these tactoids are only partially collapsed and the spacings are >1.00 nm.

Acknowledgements Help from Ms. Nadezhda Bukhanovsky (The Volcani Center, Agricultural Research Organization, Israel) in preparing and thermally treating the organoclay samples is appreciated. This research was supported by a grant from the Israeli Science Foundation (No. 919.08) and by a grant from the Ministry of Science, Culture and Sport and the Ministry of Research (Infrastructure 3-4136).

References

1. Theng BKG. The chemistry of clay-organic reactions. London: Adam Hilger; 1974.
2. Boyd SA, Chiou CT, Mortland MM. Sorption characteristics of organic compounds on hexadecyltrimethylammoniumsmectite. Soil Sci Soc Am J. 1988;52:652–60.
3. Yariv S. Introduction to organo-clay complexes and interactions. In: Yariv S, Cross H, editors. Organo-clay complexes and interactions. New York: Marcel Dekker; 2002. p. 39–111.
4. Prost R, Yaron B. Use of modified clays for controlling soil environmental quality. Soil Sci. 2001;166:880–95.
5. Churchman GJ, Gates WP, Theng BKG, Yuan G. Clays and clay minerals for pollution control. In: Bergaya F, Theng BKG,

Lagaly G, editors. Handbook of clay science. Amsterdam: Elsevier; 2006. p. 625–75.
6. Alther G. Cleaning wastewater: removing oil from water with organoclays. Filtr Sep. 2008;45:22–4.
7. Borisover M, Gerstl Z, Burshtein F, Yariv S, Mingelgrin U. Organic sorbate–organoclay interactions in aqueous and hydrophobic environments: sorbate-water competition. Environ Sci Technol. 2008;42:7201–6.
8. Zhu R, Zhu J, Ge F, Yuan P. Regeneration of spent organoclays after the sorption of organic poluttants: a review. J Environ Manag. 2009;90:3212–6.
9. Borisover M, Bukhanovsky N, Lapides S, Yariv S. Thermal treatment of organoclays: effect on the aqueous sorption of nitrobenzene on *n*-hexadecyltrimethyl ammonium montmorillonite. Appl Surf Sci. 2010;256:5539–44.
10. Borisover M, Bukhanovsky N, Lapides S, Yariv S. Mild preheating of organic cation-exchanged clays enhances their interactions with nitrobenzene in aqueous environment. Adsorption. 2010;16:223–32.
11. Dell'Abate MT, Benededetti A, Sequi P. Thermal methods of organic matter maturation monitoring during a composting process. J Therm Anal Calorim. 2000;61:389–96.
12. Green-Kelly R. The montmorillonite minerals (smectites). In: Mackenzie RC, editor. The differential thermal investigation of clays. London: Mineralogical Society (Clay Minerals Group); 1957. p. 140–64.
13. Langier-Kuzniarowa A. Thermal analysis of organo-clay complexes. In: Yariv S, Cross H, editors. Organo-clay complexes and interactions. New York: Marcel Dekker; 2002. p. 273–344.
14. Yariv S. Differential thermal analysis (DTA) in the study of thermal reactions of organo-clay complexes. In: Ikan R, editor. Natural and laboratory simulated thermal geochemical processes. Dordrecht: Kluwer Academic Publishers; 2003. p. 253–96.
15. Yariv S. The role of charcoal on DTA curves of organoclay complexes: an overview. Appl Clay Sci. 2004;24:225–36.
16. He H, Ding Z, Zhu J, Yuan P, Xi Y, Yang D, Frost RL. Thermal characterization of surfactant-modified montmorillonite. Clays Clay Miner. 2005;53:287–93.
17. Yariv S, Borisover M, Lapides S. Few introducing comments on the thermal analysis of organoclays. J Therm Anal Calorim. 2011;105:897–906.
18. Yariv S. Combined DTA-mass spectroscopy of organoclay complexes. J Therm Anal. 1990;36:1953–61.
19. Allaway WH. Differential thermal analysis of clays treated with organic cations as an aid in the study of soil colloids. Soil Sci Am Proc. 1949;13:183–8.
20. Bradley WF, Grim RE. Colloid properties of layer silicates. J Phys Chem. 1948;52:1404–13.
21. Lapides I, Borisover M, Yariv S. Thermal-analysis of hexadecyltrimethylammonium-montmorillonites. Part 1: thermogravimetry, carbon and hydrogen analysis and thermo-IR-spectroscopy-analysis. J Therm Anal Calorim. 2011;105:921–9.
22. Lapides I, Borisover M, Yariv S. Thermal-analysis of hexadecyltrimethylammonium-montmorillonites. Part 2: thermo-XRD-spectroscopy analysis. J Therm Anal Calorim. 2011;105:39–51.
23. Newman ACD, Brown G. The chemical constitutions of clays. In: Newman ACD, editor. Chemical composition of clays and clay minerals. Mineralogical society monograph No. 6. London: Longman Scientific and Technical; 1987. p. 1–128.
24. Yariv S, Lapides I. The use of thermo-XRD-analysis in the study of organo-smectite complexes. J Therm Anal Calorim. 2005;80:11–26.
25. Yermiyahu Z, Lapides I, Yariv S. Thermo-XRD-analysis of montmorillonite treated with protonated Congo-red: curve fitting. Appl Clay Sci. 2005;30:33–41.
26. Ovadyahu D, Lapides I, Yariv S. Thermal analysis of tributylammonium montmorillonite and Laponite. J Therm Anal Calorim. 2007;87:125–34.
27. Hermosin MC, Cornejo J. Binding mechanism of 2,4-dichlorophenoxyacetic acid by organo-clays. J Environ Qual. 1993;22:325–32.
28. Hermosin MC, Crabb A, Cornejo J. Sorption capacity of organoclays for anionic and polar organic contaminants. Fresenius Environ Bull. 1995;4:514–21.
29. He H, Ding Z, Zhu J, Yuan P, Xi Y, Yang D, Frost RL. Thermal characterization of surfactant-modified montmorillonite. Clays Clay Miner. 2005;53:287–93.
30. Xi Y, Frost RL, He H. Modification of the surfaces of Wyoming montmorillonite by the cationic surfactants alkyl trimethyl, dialkyl dimethyl, and trialkylmethyl ammonium bromides. J Colloids Interface Sci. 2007;305:150–8.
31. Gao Z, Xie W, Hwu JM, Wells L, Pan WP. The characterization of organic modified montmorillonite and its filled pmma nanocomposite. J Therm Anal Calorim. 2001;64:467–75.
32. Xie W, Gao Z, Pan WP, Hunter D, Singh A, Vala R. Thermal degradation chemistry of alkyl quaternary ammonium montmorillonite. Chem Mater. 2001;13:2979–90.
33. Xi Y, Martens W, He H, Frost RL. Thermogravimetric analysis of organoclays intercalated with the surfactant octadecyltrimethylammonium. J Therm Anal Calorim. 2005;81:91–7.
34. Cervantes-Uc JM, Cauich-Rodriguez JV, Vazquez-Torres H, Grafias-Mesias LF, Paul DR. Thermal degradation of commercially available organoclays studied by TGA-FTIR. Thermochim Acta. 2007;457:92–102.
35. Tiwari RR, Khilar KC, Natarajan U. Synthesis and characterization of novel montmorillonites. Appl Clay Sci. 2008;38:203–8.
36. Onal M, Sarikaya Y. Thermal analysis of some organoclays. J Therm Anal Calorim. 2008;91:261–5.
37. Earley JW, Milne IH, McVeagh WJ. Dehydration of montmorillonite. Amer Miner. 1953;38:770–83.